A Comparative Study of Nanocomposites Based on a Recycled Poly(methyl methacrylate) Matrix Containing Several Nanoclays

L. Martin,[1] G. Kortaberria,[1] A. Vazquez,[1] M. Fermeglia,[2] L. Martinelli,[3] S. Sinesi,[3] A. Jimeno,[1] K. de la Caba,[1] I. Mondragon[1]

[1]*Materials and Technologies, Group, Escuela Politécnica, Universidad del País Vasco/Euskal Herriko Unibertsitatea, 20018 Donostia, San Sebastián, Spain*

[2]*Department of Chemical Engineering–DICAMP, Computer-aided Systems Laboratory, University of Trieste, Piazzale Europa I, I-34127 Trieste, Italy*

[3]*Plast-Optics Research Center, 33020 Amaro, Italy*

Nanocomposites of recycled poly(methyl methacrylate) (PMMA) and both natural (Nanomer PGV MMT), and organically modified Nanomer I44P, Nanomer I30P and Cloisite 30B montmorillonites (O-MMT) were prepared by solution dispersion method with the use of two miscible solvents, followed by melt intercalation process in a twin-screw miniextruder. The final product has been found to show a homogeneous structure with a uniform dispersion/intercalation of the silicate layers. The effect of MMT and O-MMT layers on the properties of the nanocomposites was investigated and characterized by UV–vis spectroscopy, differential scanning calorimetry, atomic force microscopy, and mechanical testing. Higher contents of nanoclay in nanocomposites exhibited worse light transmittance capacity but higher tensile modulus. Properties of the samples depended not only on the clay contents (up to 10 wt%) but also on the clay type employed. POLYM. COMPOS., 29:782–790, 2008. © 2008 Society of Plastics Engineers

INTRODUCTION

In recent years, polymer-layered silicate nanocomposites have received great attention. This is mainly because this kind of materials could offer unique properties such as much higher modulus and heat-distortion temperature [1–5], unusual thermal stability [6–9], and excellent gas and water barrier properties [10–12] when compared with pristine polymers. One of the most promising approaches for the synthesis of these materials consists on the dispersion of an inorganic clay mineral in an organic polymer on a nanometer scale. In principle, small amounts of these nanoclays, in the range of 3–5% by weight, can provide properties comparable with those given by 20–30% of microsized fillers in conventional composites. However, to achieve such properties in nanocomposites requires high levels of dispersion of the organoclay, which is possible when good affinity between the polymer and the clay exists. When the polymer–organoclay interaction is not favorable enough to give well-exfoliated aluminosilicate platelets, then intercalated or partially exfoliated structures are usually obtained [13–22]. Numerous researchers used this concept for synthesizing nanocomposites based on epoxies [3, 5], unsaturated polyester, polystyrene [23, 24], polyimide [10, 11], polypropylene [25, 26], poly(ethylene oxide) [27], and so on.

Poly(methyl methacrylate) (PMMA) is an important member in the family of polyacrylic and methacrylic esters. It has several desirable properties, including exceptional optical clarity, good weatherability, high strength, and excellent dimensional stability. So it is used in many areas. PMMA/montmorillonite (MMT) nanocomposites have been synthesized by melt intercalation [28, 29], in situ polymerization [30, 31], suspension [32, 33], and emulsion polymerization. MMT was used directly or organically modified by organoammonium ions. Organic modification as well as the preparation method determine whether the material will be exfoliated or intercalated [34]. In addition, the possibility for reusing of this kind of

Correspondence to: Prof. Iñaki Mondragon; e-mail: inaki.mondragon@ehu.es

Contract grant sponsor: The European Union (Strep MoMo Project).
Contract grant sponsor: The Basque Government.
Contract grant sponsor: Ministerio de Ciencia y Tecnología; contract grant number: MAT2003-08125.
DOI 10.1002/pc.20438
Published online in Wiley InterScience (www.interscience.wiley.com).
© 2008 Society of Plastics Engineers

TABLE 1. Specifications of PMMA used in this study.

Designation	Tensile strength (MPa)	Elongation at break (%)	Flexural strength (MPa)	Flexural modulus (MPa)	Molecular weight (g/mol)	Light transmission (%)
Oroglas V920T	70	6	103	3300	90,000	92

materials, maintaining or even improving their properties by means of clay addition, can offer a significant added value and an important choice for industrial applications.

In this article, both unmodified (MMT) and organically modified montmorillonites (O-MMT) were used to prepare nanocomposites containing up to 10 wt% clay by solution dispersion method with the use of two miscible solvents [35] followed by melt intercalation process. Samples were extruded and injection molded to prepare samples for characterization. Thermal, dynamic mechanical, and morphological characterization of the nanocomposites is presented and the effect of the type of modification is discussed. UV–vis analysis, dynamic mechanical analysis (DMA), atomic force microscopy (AFM), and mechanical analysis were used for the characterization of nanocomposites.

EXPERIMENTAL

Materials

Four MMTs were used in this work. Nanomer PGV, a natural MMT (cation exchange capacity of 145 mequiv/100 g clay), Nanomer I30P, natural MMT organically modified with octadecylamine, and Nanomer I44P, organically modified with dimethyl dialkyl (C14-18) ammonium, supplied by Nanocor, and Cloisite 30B, an organically modified natural MMT, purchased from Southern Clay Products Inc. modified with a quaternary organoammonium ion, $N^{+}(CH_2CH_2OH)_2(CH_3)T$, where T represents tallow (~65% C18, ~30% C16, and ~5% C14). The cation exchange capacity of this MMT is 90 mequiv/100 g clay.

FIG. 1. Relative variation of opacity of PMMA/MMT nanocomposites with clay content under comparable processing conditions.

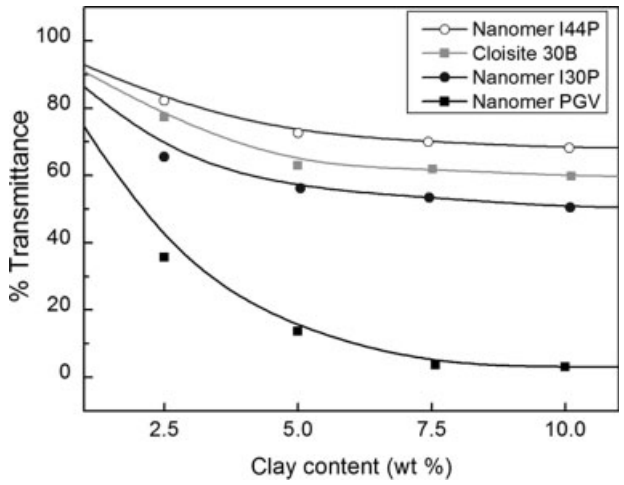

FIG. 2. Variation of transparency percent of PMMA/MMT nanocomposites with clay content as analyzed by UV–vis spectroscopy.

Recycled PMMA Oroglas V920T provided by Atoglas was used as matrix. The specifications of this material are described in Table 1. Ethanol (96%, Panreac) and dichloromethane (stabilized with amylene, Panreac) were used as solvents. An important characteristic of the used PMMA is that it has been recycled from automotive industrial rejects, being one of the components of the car lighters. Consequently, one of the most important objectives of this work was to obtain transparent composites from this material, maintaining or even improving mechanical properties.

Sample Processing

Clays were dispersed by sonication in one of the solvents (ethanol) while recycled PMMA was solved in the second one (dichloromethane), miscible with the former. Both solutions were mixed and PMMA nanocomposite was precipitated after evaporation of its solvent; then, the rest of solvent was removed under vacuum. Polymer composites with different clay contents (2.5, 5, 7.5, and 10 wt%) were extruded at 180°C for 10 min with a screw rate of 100 rpm, using counter-rotating screws in asynchronous operation during 5 min, in a MiniLab Haake Rheomex CTW5 and extruding very small amounts of material (about 5–7 cm^3 depending on the density of the sample). By an integrated back flow channel the filled-in sample can be recirculated several times before being extruded through a die by a pneumatically controlled bypass. This microcompounder has a single heating zone that is preset to the desired temperature prior to extrusion. All materials were previously dried 48 h at 110°C in a vacuum oven. The nanocomposites prepared were then molded into sheets of 1 mm thickness in a Haake MiniJet system, a piston injection machine with a reduced cylinder volume, in which only a small quantity of material is required. Processing conditions were the following: an injection temperature of 180°C, a mold temperature of 105°C, an injection pressure of 900 bar (during 10 s), and a postinjection pressure of 350 bar (5 s), followed by cooling to room temperature. Sheets were prepared in a mould with DMA bar shape (60 × 10 × 1 mm^3) for structural characterization.

Characterization Techniques

UV–vis spectroscopy of the nanocomposites was performed on a Milton Roy Spectronic Genesys 5 UV–vis analyser at 680 nm wavelength. The resolution of the equipment for the wavelength range was about 5 nm. The specimens for these measurements had a thickness of ≈1 mm.

Differential scanning calorimetry scans were performed on a Mettler 822 DSC, from 30 to 180°C with a 10°C/min heating rate. Glass transition temperatures (T_g) were measured by drawing appropriate tangents at the onset of the corresponding peak.

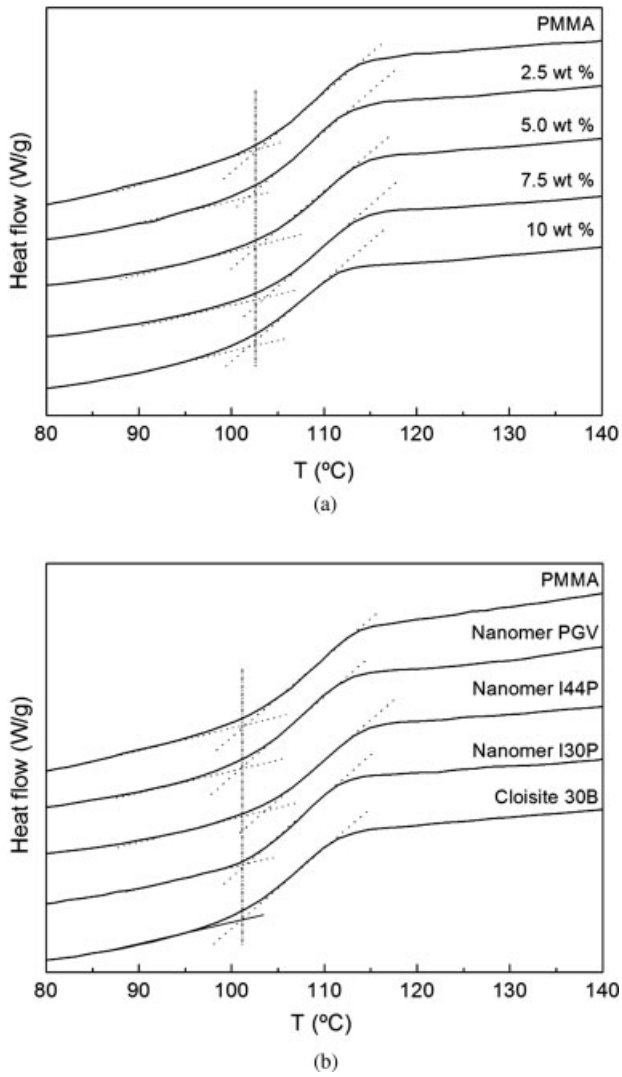

FIG. 3. (a) DSC analysis of PMMA/MMT I44P nanocomposites with several clay contents. (b) DSC analysis of nanocomposites containing 5 wt% of different clays.

DOI 10.1002/pc

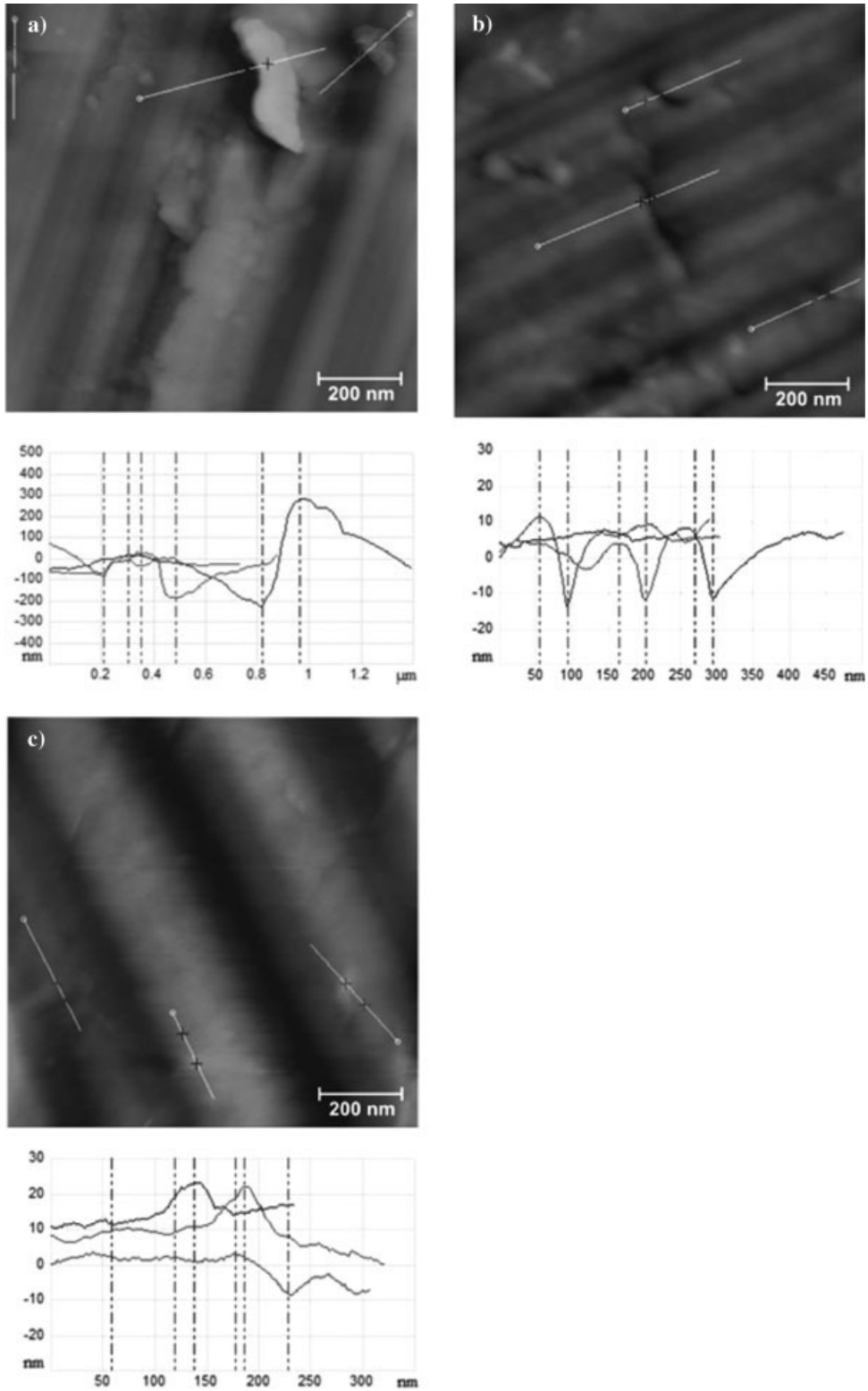

FIG. 4. AFM height images of PMMA nanocomposites with 5 wt% clay: (a) Nanomer PGV, (b) Nanomer I44P, and (c) Nanomer I30P. The projections of the surface along the white line are displayed in the form of line spectra. Distance between marks in height images are represented as dash-dot lines in spectra.

In the morphological analysis, ultrathin sections of the composites with a thickness of ~50–80 nm were cut with a Leica Ultramicrotome Ultracut R equipped with a diamond knife at room temperature. These thin cross sections were cut in order to obtain an appropriate surface for analysis by AFM. This analysis was performed on a

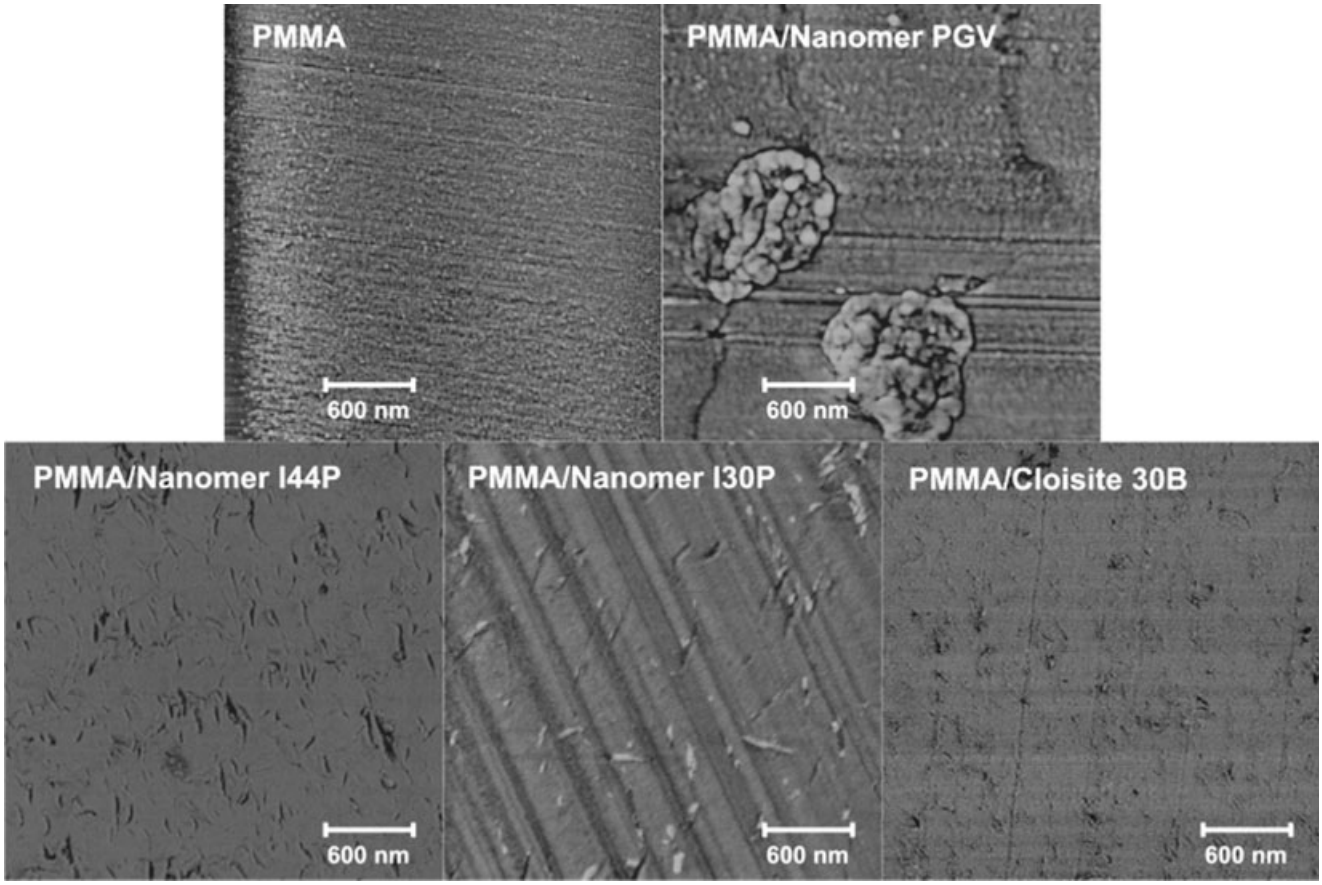

FIG. 5. AFM phase images of PMMA nanocomposites containing 5 wt% of different clays.

NanoScope IIIa multimode AFM (Digital Instruments, DI), operated in tapping mode. A J-scanner was used with commercially available silicon nanoprobes. Height and phase images were acquired simultaneously.

Mechanical analysis was made at room temperature according to ASTM D 790M for tensile tests to determine the elastic modulus from the initial part (at deformation between 0.1 and 0.3%) of stress–strain curves using an Instron, model 4206. Typically, data from five specimens were averaged to determine properties with error limits of 4% for modulus.

RESULTS AND DISCUSSION

Figure 1 shows a comparative study of the optical transparency for all analyzed nanocomposites. Samples were straight forward taken from the miniextruder. As can be seen, an increment of the percentage of clay in the composite leads to an increase in the opacity. This behavior is more evident in the case of the unmodified clay. The nanocomposites cast with organically modified clays were transparent up to clay contents of 5 wt% or even higher.

Light transmittance of nanocomposites was also investigated by UV–vis spectroscopy. When the incident light direction is perpendicular to the sample, the light transmittance of the material, $T(\lambda)$, at a wavelength, λ, is given by [36]

$$T(\lambda) = \left[1 - \frac{n^0(\lambda) - 1}{n^0(\lambda) + 1}\right] \exp(-\lambda L)$$

where α is the loss factor, $n^0(\lambda)$ is the refractive index at wavelength λ, and L is the thickness of the material.

The light transmittance curves of nanocomposites are shown in Fig. 2, being the results in agreement with those in Fig. 1. For the same clay content, the light transmittance is nearly similar for all the nanocomposites containing organoclays, although Nanomer I44P nanocomposites have a slightly higher light transmittance than the others. In all cases the level of transparency drops with clay content, but for unmodified PMMA/PGV nanocomposites the opacity appears at much lower clay contents than for the others. These results indicate that clay content has an important effect on the transparency of the nanocomposites, also playing an important role the type of clay modification employed [37].

DSC analysis has been carried out by dynamical scans from 30 to 180°C with a heating rate of 10°C/min. Figure 3a shows thermal scans for samples modified with different amounts of Nanomer I44P. The obtained T_g values, around 108°C, are very similar for all the nanocompo-

 DOI 10.1002/pc

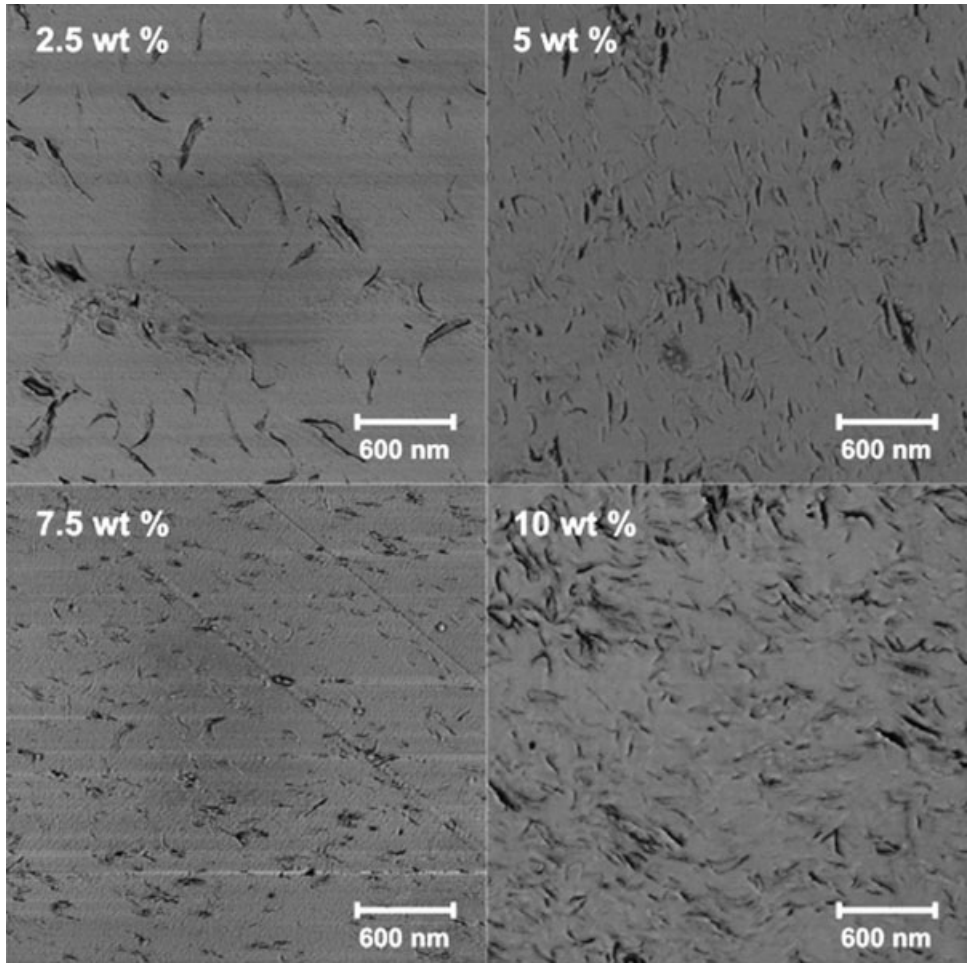

FIG. 6. AFM phase images of PMMA nanocomposites with 0, 2.5, 5, and 10 wt% I44P.

sites. Only a slight decrease of that value can be observed for the samples with the higher clay amount. This slight decrease in the T_g has been observed for all types of clays employed. Results for all the nanocomposites containing 5 wt% clay are presented in Fig. 3b. Though no significant T_g variations can be observed from one to the other nanocomposite, it is worth noting that the nanocomposite with higher transparency also shows a higher T_g, possibly as a consequence of higher extent of interactions between the modified clay and recycled PMMA.

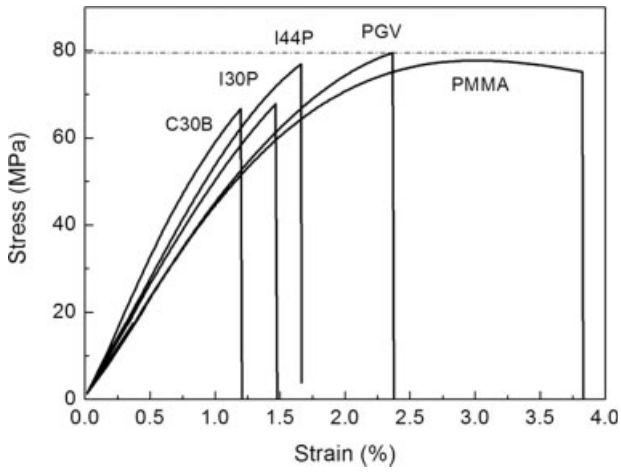

FIG. 7. Stress–strain curves on PMMA nanocomposites containing 5 wt% of different clays.

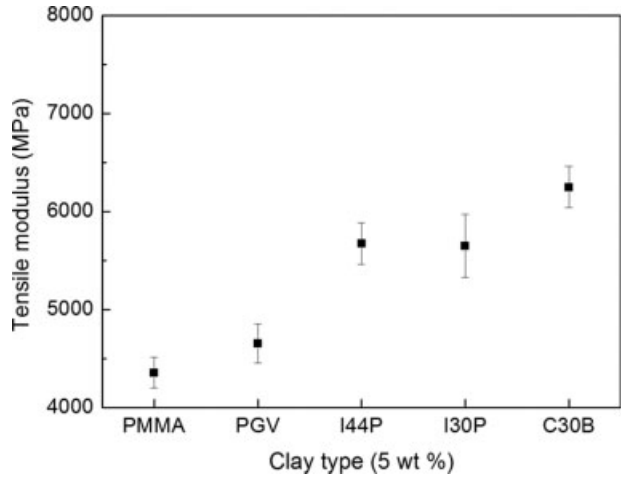

FIG. 8. Tensile modulus versus used clay for all 5 wt% contents.

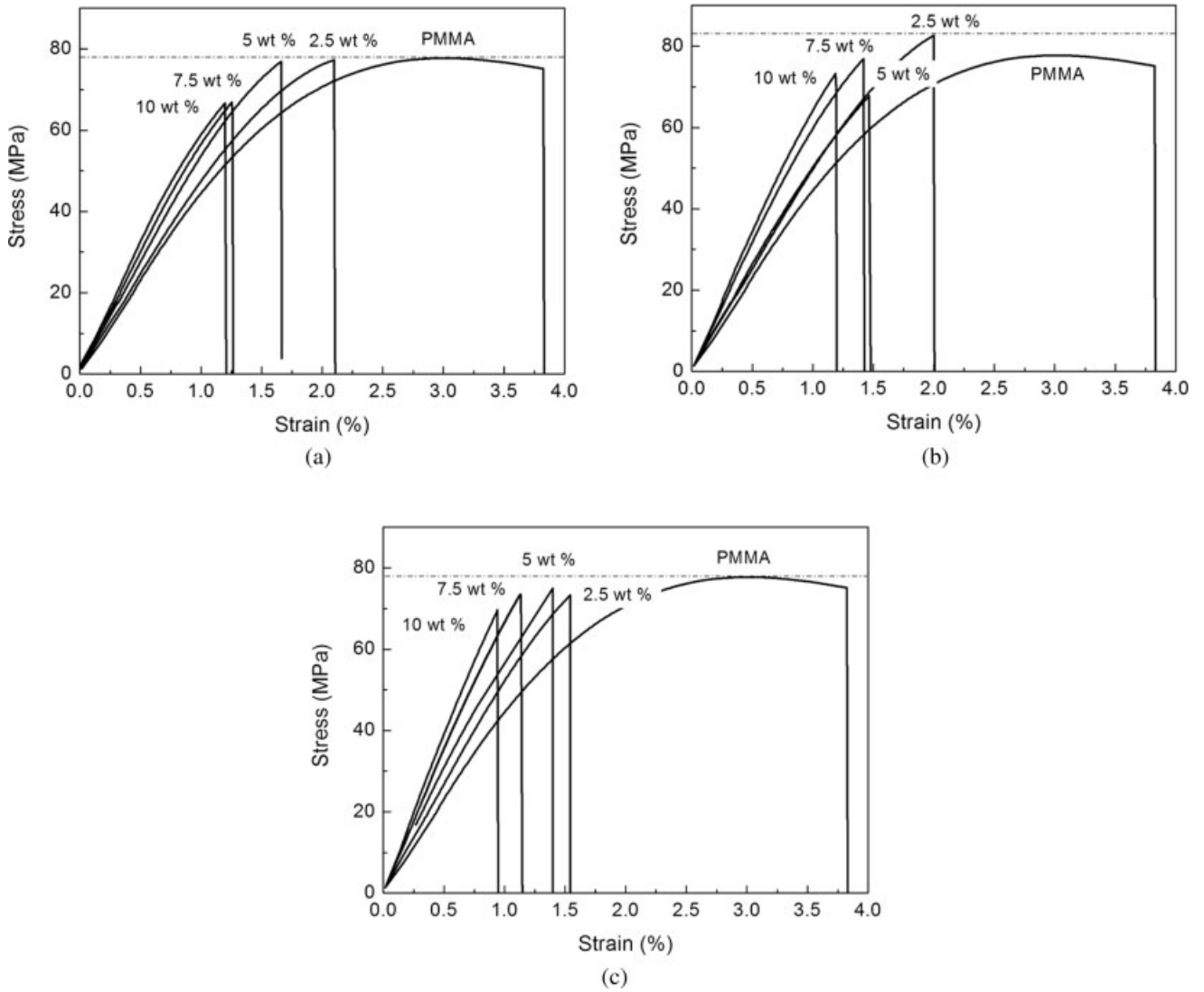

FIG. 9. Stress–strain curves for PMMA nanocomposites with different clay contents: (a) Nanomer I44P, (b) Nanomer I30P, and (c) Cloisite 30B.

Figure 4a–c show AFM micrographs of nanocomposites containing 5 wt% of different nanoclays. In the case of PMMA/unmodified clay composite (Fig. 4a), big tactoids can be observed when compared with nanocomposites with modified MMTs. The aggregates can reach dimensions up to 200 nm, as can be seen in the micrograph and the profiles obtained from the lines shown. For nanocomposites made with organically modified MMTs, some intercalated layers and small clay aggregates appear. The dark lines, measured in Fig. 4b, are cross sections of silicate layers with a thickness between 20 and 30 nm, which correspond with the size of several tens of parallel stacked silicate layers for the case of nanocomposites with Nanomer I44P, and with slightly lower dimensions for nanocomposites with Nanomer I30P (Fig. 4c). The corresponding profiles are also a demonstrator of these sizes. Phase images at higher scale are presented in Fig. 5 for nanocomposites containing 5 wt% MMT. They show a homogeneous distribution of the clays, except for the unmodified MMT, which is in agreement with the evolution of transparency degree and light transmission shown above, thus outlining the importance of the organic modification of MMTs for increasing the intercalation/exfoliation and also dispersion into the matrix. Figure 6 shows, at the same scale, a comparative of Nanomer I44P nanocomposites with different clay contents. Samples show a homogeneous distribution even for 10 wt% MMT, which allows a good transparency degree, which decreases with clay content.

Fillers are used extensively to improve mechanical properties of polymers such as stiffness, strength, and hardness. These properties usually increase with increase in the amount of fillers. Figure 7 shows the effect of clay type on stress–strain curves of nanocomposites containing 5 wt% of different clays. Tensile modulus of nanocomposites can be observed in detail in Fig. 8. Depending on the clay, there is an increase of the modulus in the range of 30–40% for nanocomposites modified with O-MMT. When the increase in the modulus value for the organi-

 DOI 10.1002/pc

cally modified MMT is compared with that of the neat PMMA and PMMA modified with unmodified MMT, this result becomes more evident. This is important taking into account that the used PMMA is recycled, which along with the transparency of the samples, gives the opportunity to recycle the material, obtaining nanocomposites that could be used not only in applications similar to those in which the matrix is used, but also in those applications with higher mechanical requirements. These results are in agreement with those from the morphological analysis shown above, wherein the unmodified clay induced the system to present a much higher amount and also size of tactoids, and consequently a worse dispersion of the clay.

Figure 9a–c shows the effect of the clay amount in each nanocomposite on the stress–strain curves. A significant gradual increase in tensile modulus is observed with clay content. This effect can be seen in more detail in Fig. 10, in which a 50–70% increase in modulus values can be observed. There is a steady increase even with the highest amount of clay (10 wt%), indicating that the route used by solution dispersion and melt intercalation leads to a good dispersion of the clays at nanoscale. Indeed, dispersion is a key factor controlling mechanical properties in this kind of materials. Unfortunately, as shown in Fig. 11, though stiffness increase is produced by increasing the clay content, the brittleness of the nanocomposites becomes higher with irregular breakage where jagged and rough surfaces are dominant. Tensile strength and strain of these materials decrease considerably with the use of modified MMTs and even more in the case of nanocomposites prepared with Cloisite 30B. Therefore, in order to maintain fracture toughness of the pristine matrix, other ways of modification seem to be needed. Work is in progress for stiffness increase of PMMA and polymer modification using modified clays in order to retain the deformability of the pristine matrix.

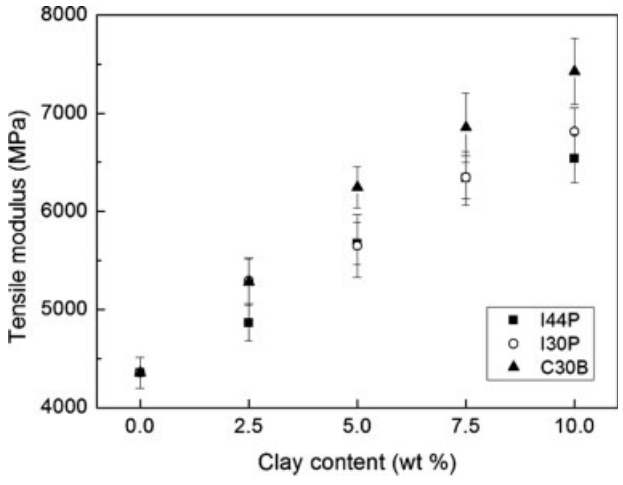

FIG. 10. Tensile modulus vs clay content for PMMA nanocomposites with different clays: Nanomer I44P, Nanomer I30P, and Cloisite 30b.

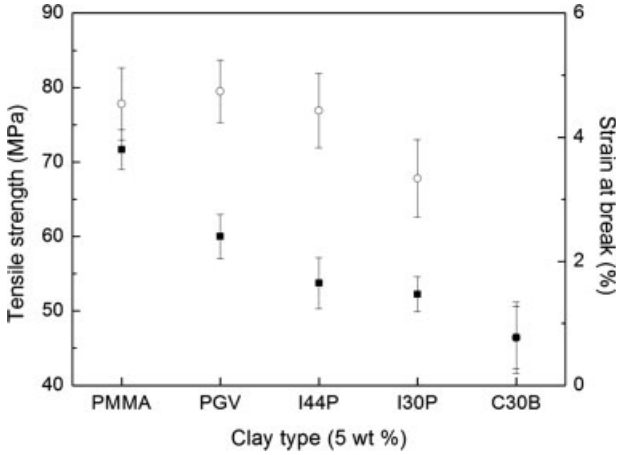

FIG. 11. Tensile strength and strain versus used clay type for 5 wt% contents.

CONCLUSIONS

The effect of morphology on optical transparency of recycled PMMA/clay nanocomposites with several organically modified clays and different clay contents has been investigated. Results show that the morphology and composition of the nanocomposites have an important influence on light transmittance of nanocomposites. With a higher dispersion degree, nanocomposites appear to show higher transparency extent. There is no improvement of thermal properties of nanocomposites, with respect to the matrix, being this fact important in order to use these materials at least in the same conditions than the matrix. Finally, mechanical testing shows that tensile modulus is increased with clay content for all the clays, which, together with the maintenance of transparency and thermal properties of the pristine matrix, allows recycling of the matrix for preparing nanocomposites with interesting properties. More work has to be performed for retaining the deformability of the polymeric matrix when clays are used for modification.

REFERENCES

1. Y. Kojima, A. Usuki, M. Kawazumi, A. Okada, T. Karauchi, and O. Kamigaito, *J. Polym. Sci. Part A: Polym Chem.*, **31**, 1755 (1993).
2. L. Liu, Z. Qi, and X. Zhu, *J. Appl. Polym. Sci.*, **71**, 1133 (1999).
3. Y. Ke, C. Long, and Z. Qi, *J. Appl. Polym. Sci.*, **71**, 1139 (1999).
4. N. Harotaka, H. Okamoto, M. Kawasumi, and A. Usuki, *J. Appl. Polym. Sci.*, **74**, 3359 (1999).
5. P.B. Messersmith and E.P. Giannelis, *Chem. Mater.*, **6**, 1719 (1994).
6. S. Wang, C. Long, X. Wang, Q. Li, and Z. Qi, *J. Appl. Polym. Sci.*, **69**, 1557 (1998).
7. D.C. Lee and L.W. Jang, *J. Appl. Polym. Sci.*, **61**, 1117 (1996).

8. M. Biwas and S.S. Ray, *J. Appl. Polym. Sci*., **77**, 2948 (2000).
9. C. Wang and T.J. Pinnavaia, *Chem. Mater*., **10**, 3769 (1998).
10. Z. Zhu, Y. Yang, J. Yin, X. Wang, Y. Ke, and Z. Qi, *J. Appl. Polym. Sci*., **73**, 2063 (1999).
11. K. Yano and A. Usuki, *J. Appl. Polym. Sci*., **31**, 2493 (1993).
12. G. Chen, K. Yao, and J. Zhao, *J. Appl. Polym. Sci*., **73**, 425 (1999).
13. M. Alexandre and P. Dubois, *Mater. Sci. Eng*., **28**, 1 (2000).
14. N. Furuichi, Y. Kurokawa, K. Fujita, A. Oyo, H. Yasuda, and M. Kiso, *J. Mater. Sci*., **31**, 4307 (1996).
15. Y. Kurokawa, H. Yasuda, M. Kashiwagi, and A. Oyo, *J. Mater. Sci. Lett*., **16**, 1670 (1997).
16. P. Adanda and E. Ruiz-Hitzky, *Chem. Mater*., **4**, 1395 (1992).
17. R.A. Vaia, S. Vasudevan, W. Krawiec, L.G. Scanlon, and E.P. Giannelis, *Adv. Mater*., **7**, 154 (1995).
18. R.A. Vaia, B.B. Sauer, O.K. Tse, and E.P. Giannelis, *J. Polym. Sci. Part B: Polym. Phys*., **35**, 59 (1997).
19. J.T. Yoon, W.H. Jo, M.S. Lee, and M.B. Ko, *Polymer*, **42**, 329 (2001).
20. J. Huang, Z. Zhu, X. Qian, and Y. Sun, *Polymer*, **42**, 873 (2001).
21. M. Zanetti, G. Camino, R. Thomann, and R. Mulhaupt, *Polymer*, **42**, 4501 (2001).
22. M. Alexandre, G. Beyer, C. Henrist, R. Cloots, A. Rulmont, R. Jerome, and P. Dubois, *Macromol. Rapid. Commun*., **22**, 643 (2001).
23. X. Kommann, L. Berglund, J. Sterte, and E.P. Giannelis, *Polym. Eng. Sci*., **38**, 1351 (1998).
24. W. Xie, J.M. Hwu, G.J. Jiang, T. Buthelezi, and W.P. Pan, *Polym. Eng. Sci*., **43**, 214 (2003).
25. P. Maiti, P.H. Nam, M. Okamoto, N. Hasegawa, and A. Usuki, *Macromolecules*, **35**, 2042 (2002).
26. J. Ma, Z. Qi, and Y. Hu, *J. Appl. Polym. Sci*., **82**, 3611 (2001).
27. Z. Shen, G.P. Simon, and Y.B. Cheng, *Polym. Eng. Sci*., **42**, 2369 (2002).
28. N. Moussaif and G. Groeninckx, *Polymer*, **44**, 7899 (2003).
29. D. Wang, J. Zhu, Q. Yao, and C.A. Wilkie, *Chem. Mater*., **14**, 3837 (2002).
30. X. Qu, T. Guan, G. Liu, Q. She, and L. Zhang, *J. Appl. Polym. Sci*., **97**, 348 (2005).
31. X.Y. Huang and J. William, *Macromolecules*, **34**, 3255 (2000).
32. H. Essawy, A. Badran, A. Youssef, and A.E. El-Hakim, *Polym. Bull*., **53**, 9 (2004).
33. Y.S. Choi, M.H. Choi, K.H. Wang, S.O. Kim, Y.K. Kim, and J. Chung, *Macromolecules*, **34**, 8978 (2001).
34. T. Peprnicek, J. Duchet, L. Kovarova, J. Malac, J.F. Gerard, and J. Simonik, *Polym. Degrad. Stab*., **91**, 1855 (2006).
35. B. Pourabas and V. Raeesi, *Polymer*, **46**, 5533 (2005).
36. D. Yuming, G. Aijuan, and F. Zhengping, *Polym. Int*., **53**, 85 (2004).
37. P. Kampeerapappun, D. Aht-ong, D. Pentrakoon, and K. Srikulkit, *Carbohydr. Polym*., **67**, 155 (2007).
38. E.P. Giannelis and B. Messersmith, U. S. Patent W096/08526 (1996).

 DOI 10.1002/pc